Aggregation–Dissociation Studies of Asphaltene Solutions in Resins Performed Using the Combined Freeze Fracture –Transmission Electron Microscopy Technique

ARTICLE *in* ENERGY & FUELS · JUNE 2008

Impact Factor: 2.79 · DOI: 10.1021/ef800108p

2 AUTHORS, INCLUDING:

Socrates Acevedo
Central University of Venezuela
111 PUBLICATIONS **1,265** CITATIONS

Aggregation−Dissociation Studies of Asphaltene Solutions in Resins Performed Using the Combined Freeze Fracture−Transmission Electron Microscopy Technique

Socrates Acevedo* and Clara Zuloaga

Universidad Central de Venezuela, Facultad de Ciencias, Escuela de Química, 40756 Caracas, 1053 Venezuela

Pedro Rodríguez

Universidad Central de Venezuela, Facultad de Ciencias, Centro de Microscopía Electrónica, 40756 Caracas, 1053 Venezuela

Received February 13, 2008. Revised Manuscript Received April 22, 2008

Solutions of asphaltenes in resins (3%) were studied combining the freeze fracture and transmission electron microscopy techniques (FF-TEM). These studies were performed by analyzing samples prepared at different temperatures (T) from 25 up to 250 °C. In this temperature range, mean particle diameters (D_p) were found to drop from about 5 to about 3.5 nm. The smallest diameter measured at each temperature (D_S) reached a constant value equal to 2.5 nm in the range between 100 and 250 °C. Frequencies $f(D)$ of all but D_S values were found to decrease at some temperatures reveling that diameters $D > D_S$ correspond to aggregates (Ag). Moreover, during this heating, we found that whereas for big (B) and smallest diameters frequencies $f(D)$ either decrease (big) or increase (D_S) continuously, maxima were found for intermediate (I) diameters. This suggests that under the conditions of this experiment (temperature and time) conversion from intermediate to smallest diameter meets some energy barrier high enough for the accumulation of intermediate size diameters. These results were interpreted in terms of the consecutive process $\mathrm{Ag(B)} \xrightarrow[T]{k_1} \mathrm{Ag(I)} \xrightarrow[T]{k_2} \mathrm{A1M}$ where A1M stand for A1-type molecules and $k_1 > k_2$; consequently, because of the low solubility of A1M, conversion from intermediate aggregates to molecules is a difficult step. The above results and many others in the literature are in agreement with the colloidal, solubility, and aggregates hypothesis related to A1 and A2 fractions of asphaltenes.

Introduction

Asphaltenes, defined as the toluene soluble and heptane insoluble fractions of crude oil, are the most studied material of petroleum. There are at least two reasons for the interest in these compounds: one is the negative impact they have on many important industrial operations where many problems in production (plugging of production facilities due to phase separation), transportation (deposition of asphaltic material on transportation lines), catalyst fouling during oil refining among others are promoted by asphaltene; the other is the interesting physical and chemical behavior displayed by this sample under many (if not all) conditions used to study them.

Aggregation is by far, the most important characteristic of asphaltenes as can be assessed in the literature reviewed below where all citations deals directly or indirectly with it; this is because of the impact it has on both academic and industrial fields. Colloidal flocculation during production operations, wettability changes in oil reservoirs, water-in-oil emulsion formation, colloidal sedimentation during storage and transportation, and coke and solid formation during refining and catalyst fouling are all related to aggregation of asphaltenes in crude oil. Research conducted this far, some of which is reviewed below, has reveled that the main driving force for aggregation are van der Waals, polar, and hydrogen bonding forces, which, for asphaltene molecular mass, could lead to very high energy values. Thus, in solvents like toluene, aggregation begins at extremely low concentrations.[1–4] Aggregation at very low concentration in this and other solvents like pyridine[5,6] and *N*-methyl-2-pyrrolydinone (NMP)[7] could be expected in view of the very low solubility of fraction A1. Therefore, the opposite process: dissociation of A1-type aggregates (A1A) to afford A1-

* Corresponding author. E-mail: soaceved@cantv.net.

(1) Acevedo, S.; Ranaudo, M. A.; Pereira, J. C.; Castillo, J.; Fernández, A.; Pérez, P.; Caetano, M. Thermo-optical studies of asphaltene solutions: Evidence for solvent-solute aggregate formation. *Fuel* **1999**, *78*, 997–1003.

(2) Andreatta, G.; Goncalves, C. C.; Buffin, G.; Bostrom, N.; Quintella, C. M.; Arteaga-Larios, F.; Perez, E.; Mullins, O. C. Nanoaggregates and Structure-Function Relations in Asphaltenes. *Energy Fuels* **2005**, *19* (4), 1282–1289.

(3) Evdokimov, I. N.; Eliseev, N. Y.; Akhmetov, B. R. Asphaltene dispersions in dilute oil solutions. *Fuel* **2006**, *85* (10 and 11), 1465–1472.

(4) (a) Andrews, A. B.; Guerra, R. E.; Mullins, O. C.; Sen, P. N. Diffusivity of Asphaltene Molecules by Fluorescence Correlation Spectroscopy. *J. Phys. Chem. A.* **2006**, *110* (26), 8093–8097. (b) Schneider, M. H.; Andrews, A. B.; Mitra-Kirtley, S.; Mullins, O. C. Asphaltene Molecular Size by Fluorescence Correlation Spectroscopy. *Energy Fuels* **2007**, *21* (5), 2875–2882.

(5) Sheu, E. Y. Petroleum Asphaltene-Properties, Characterization, and Issues. *Energy Fuels* **2002**, *16* (1), 74–82.

(6) Norinaga, K.; Wargardalam, V. J.; Takasugi, S.; Iino, M.; Matsukawa, S. Measurement of Self-Diffusion Coefficient of Asphaltene in Pyridine by Pulsed Field Gradient Spin-Echo 1H NMR. *Energy Fuels* **2001**, *15* (5), 1317–1318.

(7) Badre, S.; Carla Goncalves, C.; Norinaga, K.; Gustavson, G.; Mullins, O. C. Molecular size and weight of asphaltene and asphaltene solubility fractions from coals, crude oils and bitumen. *Fuel* **2006**, *85* (1), 1–11.

10.1021/ef800108p CCC: $40.75

ohio2/yef-yef/yef-yef/yef99907/yef2932d07z | xppws | 23:ver.3 | 6/7/08 | 22:03 | Msc: ef-2008-00108p | TEID: kkt00 | BATID: ef5a04

type molecules (A1M) is expected to be a difficult step as found in the present research (see below).

As reported by Acevedo et al.[8,9] using the *para*-nitrophenol method (PNP) asphaltenes were fractionated in fractions A1 and A2 where fraction A2 has the usual asphaltene solubility (about 57 to 100 g L^{-1}, depending on sample; toluene, room temperature). However, under the same conditions, fraction A1 has a very low solubility close to 0.09 g L^{-1}. In other words, though the entire sample (asphaltene) has a known solubility in toluene, it does contain substantial amounts (50% or more) of the very low soluble fraction A1. This finding (among other things) leads to the proposition of the A1-type aggregates or colloids (A1A) where the core is occupied by A1M and the periphery by A2M and solvent media.

Hence, in view of the fact the very low solubility of A1, aggregation of asphaltenes at very low concentration in both polar and nonpolar solvents is predictable and this, along with other asphaltene features, was thoroughly discussed previously.[9] For instance, asphaltene aggregates of A1 dispersed by the soluble components of fraction A2 could be expected in toluene and other more polar solvents such as pyridine and NMP. The large difference in solubility has been accounted for in terms of rigid or *continental*-type structures for A1M and flexible or *archipelago*- or *rosary*-type structures for A2-type molecules (A2M).[9] As predicted by molecular mechanics calculations, these basic differences could lead to solubility parameter differences consistent with the solubility difference found.[9,40] From a molecular perspective, rigid A1M could interact efficiently with each other leading to large solubility parameter differences with the solvent and hence to very low solubility; on the contrary, flexible A2M (many conformers are possible) leads to solubility parameter similar to the solvent and high solubility[9,40]

Of course, formations of colloidal solutions have the same origin described above for aggregates where colloids are structured by an insoluble core surrounded by a soluble periphery.[8,9] As reported many times in the literature, aggregation of these colloids leads to flocks having fractal structures.[5,12,29,33]

In the following review and when convenient, we have used italics to distinguish literature comments and results from ours.

The size and shape of asphaltene colloids and molecules have received considerable attention in the literature. Small-angle neutron scattering (SANS) has been used by Gawrys and Kilpatrick to propose an *oblate cylinder structure for asphaltenes colloids*.[10] This type of structure would probably be consistent with the continental-type model (CTM) for molecules in the A1 fraction described above.[8,9]

Image analysis methods for the study of asphaltene size and shape and asphaltene flocculation have been reported by Bybee.[11] According to this author, "*a new method was developed that uses image analysis to convert information obtained from a sequence of images to describe the process of asphaltene precipitation under reservoir conditions. The full-length paper describes application of frequency−domain imaging to study the asphaltene-precipitation/-flocculation/-deposition process for a CO_2 miscible flood*".[11]

The importance of colloidal characteristics in field operations was highlighted in a recent review by Sheu[44] where links between colloidal dimension of asphaltenes and parameters used in field operations were explored suggesting that methods such as small angle X-ray scattering (SAXS) and small angle neutron scattering (SANS) are *legitimate* in this regard.

Pulsed field gradient spin echo nuclear magnetic resonance (PFG-SE NMR) has been used by Oštlund et al. to study the self-diffusion of asphaltenes in deuterated toluene.[13] The authors reported a diffusion coefficient of 2.2×10^{-10} at infinite dilution. According to them, "*both asphaltene and toluene diffusion indicates that asphaltenes have a disk-like shape as revealed by a strong concentration dependence on the diffusion coefficients*". As mentioned above, disk or oblate shaped structures are consistent with A1M or CTM.

A study of asphaltene aggregation in toluene solutions using confocal microscopy was used by Castillo et al.[14] According to these authors, "*flock growing process and flock characteristics depend on crude oil nature*". Wettability studies on mica surfaces exposed to crude oils using AFM, were reported by Buckley and Lord.[15] Using the three phase method (water/crude/mica), they reported the formation of organic coatings with variable thickness. According to them, "*weakly water-wet systems exhibited many surface features, but the waiting tended to be unstable and to detach from the surface, especially during AFM scanning in water. The most oil-wet systems exhibited thick, stable organic coatings that were not disturbed by AFM scanning*".[15]

Some SAXS and SANS results reported for asphaltenes were questioned by Sirota,[16] because according to him, "*some scattering used to propose the presence of nanometer scale colloids, is likely to be the result of heterogeneities similar to those observed in any one-phase liquid mixture of unlike molecules*". Maybe the so-called *heterogeneities* are due to crystallike stacks of A1M (see the comments of ref 18 below).

SAXS, SANS, and dynamic light scattering methods were used by Espinat et al. to study the temperature dependence of asphaltene aggregate sizes in toluene solutions.[17] According to them: *A large range of aggregate sizes is covered by combining the three scattering methods. The effect of temperature on aggregate size was also investigated over a considerable temperature range. A huge modification of asphaltene macrostructure was observed. At high temperatures, reversible aggregation of asphaltene leads to stable small entities. When decreasing the temperature, irreversible aggregation of asphaltene occurs, corresponding to a large increase of the*

(8) Gutierrez, L. B.; Ranaudo, M. A.; Méndez, B.; Acevedo, S. Fractionation of asphaltene by complex formation with *p*-nitrophenol. A method for structural studies and stability of asphaltene colloids. *Energy Fuels* **2001**, *15*, 624–628.

(9) Acevedo, S.; Castro, A.; Negrin, J. G.; Fernández, A.; Escobar, G.; Piscitelli, V.; Delolme, F.; Dessalces, G. Relations between Asphaltene Structure and Their Physical and Chemical Properties. The Rosary Type Structure. *Energy Fuels* **2007**, *21* (4), 2165–2175.

(10) Gawrys, K. L.; Kilpatrick, P. K. Asphaltenic aggregates are polydisperse oblate cylinders. *J. Colloid Interface Sci.* **2005**, *288* (2), 325–334.

(11) Bybee, K. A New Method to Characterize the Size and Shape Dynamics of Asphaltene Deposition. *J. Pet. Technol.* **2004**, *56* (1), 43–44.

(12) Sheu, E. Colloidal properties of asphaltenes in organic solvents. *Asphaltenes: Fundamentals and Applications*; Sheu, E., Mullins, O. C., Ed.; Plenum: New York, 1999.

(13) Östlund, J.-A.; Andersson, S.-I.; Nydén, M. Studies of asphaltenes by the use of pulsed-field gradient spin echo NMR. *Fuel* **2001**, *80* (11), 1529–1533.

(14) Castillo, J.; Hung, J.; Goncalves, S.; Reyes, A. Study of asphaltenes aggregation process in crude oils using confocal microscopy. *Energy Fuels* **2004**, *18* (3), 698–703.

(15) Buckley, J. S.; Lord, D. L. Wettability and morphology of mica surfaces after exposure to crude oil. *J. Pet. Sci. Eng.* **2003**, *39* (3 and 4), 261–273.

(16) Sirota, E. B. Physical structure of asphaltenes. *Energy Fuels* **2005**, *19* (4), 1290–1296.

(17) Espinat, D.; Fenistein, D.; Barré, L.; Frot, D.; Briolant, Y. Effects of temperature and pressure on asphaltenes agglomeration in Toluene. A light, X-ray, and neutron scattering investigation. *Energy Fuels* **2004**, *18* (5), 1243–1249.

ohio2/yef-yef/yef-yef/yef99907/yef2932d07z | xppws | 23:ver.3 | 6/7/08 | 22:03 | Msc: ef-2008-00108p | TEID: kkt00 | BATID: ef5a04

aggregate size. They[17] also investigated the effect of pressure on asphaltene solution in toluene as a function of temperature and concluded that *pressure has a minor effect, which is much less important than that of temperature, on the weight of the asphaltene aggregates.* The so-called *stable small entities* are probably A1M (see the Results and Experimental Details sections below).

Tanaka et al.[18] have reported X-ray diffraction (XRD) and SAXS measurements made on asphaltenes and vacuum residua isolated from three different crude oils—Maya (MY), Khafji (KF), and Iranian Light (IL)—to characterize the petroleum asphaltene aggregates present under various conditions.[18] The authors reported *interlayer distances of 3.6 Å and the staked cluster decreased in size from 8 to 5 aromatic sheets when temperature was increased from 30 to 300 °C.* On the basis of these and earlier results, a hypothetical hierarchical model of asphaltene aggregation was proposed by the authors.[18] In view of the low solubility and rigidity of A1M, formation of crystal-like stacks by them is expected.

In an attempt to characterize asphaltene solutions so to account for macroscopic properties such as viscosity and solubility, the SAXS and NMR relaxation methods were combined by Jestin and Barré.[19] Authors concluded that *no simple geometrical model for asphaltene particles could account for the results*. Perhaps these authors could have reached better conclusions had they considered the presence of both A1 and A2 fractions.

Gateau et al. used viscosity and SAXS methods to study the dilution of toluene solutions of asphaltene with polar solvents observing both a decrease of viscosity and radius of gyration.[20]

The "*state of the art*" concerning the flocculation of asphaltenes has two major sections: characterization of asphaltenes in various environments and modeling of flocculation have been described by Pina et al. in a review.[21] According to these researchers, "*the models available still require experimental data which is difficult to collect and further research is needed to improve this situation*". However, this review makes no mention of A1 and A2 fraction properties reported before the review was published.

Using a dynamic light scattering technique and a kinetic method, Marczak et al. have concluded that *the phase transition leading to asphaltene flocculation is of the liquid−liquid type and hence the flocculation process was found by them to be reversible*.[22] In this case, it would be interesting to rethink this conclusion in the light of the colloid structure in terms of A1M in the core and A2M in the periphery of colloids.

An analytical solution of the associative Ornstein−Zernike integral equation in the Percus−Yevick approximation to model asphaltene structural properties and phase separation in model oil dispersions as a function of pressure, temperature, and composition was reported by Lira-Galeana and Duda using a *hard sphere approach for asphaltenes and a hard spheres flexible linear chains model for solvent. The authors concluded that their theoretical results compare well with experimental evidence*.[23] The connection between *hard sphere* and rigid core (A1) and *hard spheres flexible linear chains model for solvent* and flexible A2M in the periphery are evident in this model.

The size of asphaltene flocculates in toluene and toluene−*n*-heptane mixtures, using the light-scattering technique was measured by Rajagopal and Silva.[24] *Sizes were measured for a period of about 10000 min at a constant temperature of 20 °C*. They found that the average size of the particles remained constant with time and increase with an increase in amount of *n*-heptane.[24] Large asphaltenes aggregates were observed by Perez-Hernández et al., in vacuum residues using both scanning and transmission electron microscopy.[25] Using SAXS, Sheu and Acevedo[26] reported colloidal diameters near 7 nm for Furrial crude oils.

A minimum in the intrinsic viscosity was found by Fenistein et al.,[27] when diluted toluene solutions of asphaltenes were treated with heptane. According to these authors,[27] the intrinsic viscosity increased again near the flocculation point.

Barré et al., using SANS, analyzed several asphaltene solutions in toluene and found an average radius in the 0.63−1.8 nm range.[28] Liu and Sheu reported fractal structures for asphaltene in toluene solutions.[29] Fotland[30] reported a conductivity method for detecting asphaltene precipitation under high pressure and high temperature. Bardon et al.,[31] using SAXS, SANS, and toluene solutions of asphaltenes and resins, found radii between 0.8 and 20 nm for asphaltene particles considered as thin disks (between 0.8 and 1 nm thick). The authors[31] reported that the maximum radius decreased with resin content. Storm et al.[32] reported size particles on the order of 10 nm for a VR analyzed by SAXS. *They*[32] *found that asphaltene particles are stabilized below 200 °C against the attractive dispersion forces between asphaltenes by an adsorbed layer of non-asphaltenic molecules (NAM).* These authors estimated that the binding energy holding these NAM to the particle is about *3 kT*.

(18) Tanaka, R.; Sato, E.; Hunt, J. E.; Winans, R. E.; Sato, S.; Takanohashi, T. Characterization of asphaltene aggregates using X-ray diffraction and small-angle X-ray scattering. *Energy Fuels* **2004**, *18* (4), 1118–1125.

(19) Jestin, J.; Barré, L. Application of NMR solvent relaxation and SAXS to asphaltenes solutions characterization. *J. Dispersion Sci. Technol.* **2004**, *25* (3), 341347.1.

(20) Gateau, P.; Hénaut, I.; Barré, L.; Argillier, J. F. Heavy oil dilution oils. *Oil Gas Sci. Technol.* **2004**, *59* (5), 503–509.

(21) Pina, A.; Mougin, P.; Béhar, E. Characterization of asphaltenes and modeling of flocculation - State of the art. *Oil Gas Sci. Technol.* **2006**, *61* (3), 319–343.

(22) Marczak, W.; Dafri, D.; Modaressi, A.; Zhou, H.; Rogalski, M. Physical state and aging of flocculated asphaltenes. *Energy Fuels* **2007**, *21* (3), 1256–1262.

(23) Duda, Y.; Lira-Galeana, C. Thermodynamics of asphaltene structure and aggregation. *Fluid Phase Equilib.* **2006**, *241* (1 and 2), 257–267.

(24) Rajagopal, K.; Silva, S. M. C. An experimental study of asphaltene particle sizes in n-heptane-toluene mixtures by light scattering. *Braz. J. Chem. Eng.* **2004**, *21* (4), 601–609.

(25) Pérez-Hérnandez, R.; Mendoza-Anaya, D.; Mondragón-Galicia, G.; Espinoza, M. E.; Rodríguez-Lugo, V.; Lozada, M.; Arenas-Alatorre, J. Microstructural study of asphaltene precipitated with methylene chloride and n-hexane. *Fuel* **2002**, *82*, 977–982.

(26) Sheu, E. Y.; Acevedo, S. Effect of pressure and temperature on colloidal structure of furrial crude oil. *Energy Fuels* **2001**, *15*, 236–240.

(27) Fenistein, D.; Barre, J.; Broseta, D.; Espinat, D.; Livet, A.; Roux, J. N.; Scarcella, M. Viscosimetric and neutron scattering study of asphaltene aggregates in mixed toluene/heptane solvents. *Langmiur* **1998**, *14*, 1013–1020.

(28) Barre, L.; Spinat, D.; Rosemberg, E.; Scarcella, M. Colloidal structure of heavy crudes and asphaltene solutions. *Rev. Inst. Fr. Pet.* **1997**, *52*, 161–175.

(29) Liu, Y. C.; Sheu, E. Y.; Chen, S. H.; Storm, D. A. Fractal Structure of Asphaltenes in Toluene. *Fuel* **1995**, *74* (9), 1352–1356.

(30) Fotland, P. Precipitation of asphaltenes at high pressures; experimental technique and results. *Fuel Sci. Technol. Int.* **1996**, *14* (1 and 2), 313–325.

(31) Bardon, Ch.; Barre, L.; Espinat, D.; Guille, V.; Li, M. H.; Lambard, J. C.; Ravey, J. C.; Rosemberg, E.; Zemb, T. Colloidal structure of crude oils and suspensions of asphaltenes and resins. *Fuel Sci. Tech. Int.* **1996**, *14* (1 and 2), 203–242.

(32) Storm, D. A.; Barresi, R. J.; Sheu, E. Y. Flocculation of asphaltenes in heavy oil at elevated temperaturas. *Fuel Sci. Technol.* **1996**, *14* (1 and 2), 243–260.

(33) Tanaka, R.; Hunt, J. E.; Winans, R. E.; Thiyagarajan, P.; Sato, S.; Takanohashi, T. Aggregates Structure Analysis of Petroleum Asphaltenes with Small-Angle Neutron Scattering. *Energy Fuels* **2003**, *17* (1), 127–134.

ohio2/yef-yef/yef-yef/yef99907/yef2932d07z | xppws | 23:ver.3 | 6/7/08 | 22:03 | Msc: ef-2008-00108p | TEID: kkt00 | BATID: ef5a04

Tanaka et al. examined changes in the structures of petroleum asphaltene aggregates in situ with small-angle neutron scattering (SANS).[33] *Asphaltenes were isolated from three different crude oils: Maya, Khafji, and Iranian Light. An aliquot of the 5 wt % asphaltene solution in deuterated Decalin, 1-methylnaphthalene, or quinoline was loaded in a special stainless steel cell for SANS measurements. SANS data measured at various temperatures from 25 to 350 C showed various topological features different with asphaltene or solvent species. A fractal network was formed only with asphaltene of Maya in Decalin, and it remained even at 350 C. In all of the solvents, asphaltenes aggregate in the form of a prolate ellipsoid with a high aspect ratio at 25 C and got smaller with increasing temperature. That became a compact sphere with the size of around 25 Å in radius at 350 C.* A similar hydrodynamic radius for the smallest particle was observed in this work (see the Abstract and below).

By a combination of static light scattering, optical absorption, dynamic viscosity, and NMR relaxation measurements, Evdokimov and collaborators[3] studied asphaltene solutions in toluene reporting an aggregation threshold of 10 mg/L. In agreement with the above arguments regarding A1A colloids (see above and refs 3, 8, and 9), they reported that, "'*Insoluble*' *asphaltenes are thought to form the stacked cores of colloidal particles while the more soluble asphaltene fraction may provide surrounding stabilizing shells/coronas*".[3] Similar low aggregation thresholds were reported earlier.[1,2]

Rotational diffusion determined by time-resolved fluorescence depolarization (FD) were employed by Badre et al.[7] to interrogate the absolute size of asphaltene molecules and to determine the relation of the size of the fused ring system to that of the corresponding molecule. Coal, petroleum, and bitumen asphaltenes were compared. The molecular size of coal asphaltenes obtained here by FD-determined rotational diffusion matches closely with Taylor-dispersion-derived translational diffusion measurements with UV absorption. Coal asphaltenes were found smaller than petroleum asphaltenes. *N*-Methyl pyrrolidinone (NMP) soluble and insoluble fractions were examined. According to these authors[7] NMP soluble and insoluble fractions of asphaltenes are monomeric.

Size and shape properties of asphaltenes have been reported by Mullins et al. in several papers using several techniques.[2,4,7] By working at very high dilution (below 10 mg/L), aggregation problems are overcome and according to these authors asphaltenes are monomeric, rather small particles in the 700−1000 g/mol molecular mass range forming nanoaggregates in toluene at concentrations close to 100 mg/L. Small hydronamic radios close to 10 nm were reported.[4a]

Dispersion of asphaltenes by resins is a well know phenomena which has been the subject of several studies in the past[34–38] because the role resins play in stabilizing asphaltene particles. This is confirmed by the results below (see the Discussion section).

The combined freeze fracture−transmission electron microscopy (FF-TEM) technique was employed earlier to analyze colloidal sizes in four Venezuelan crude oils.[39] Very satisfactory results were obtained, and comparison with previous SAXS results[26] was very good. These results[39] motivated the present study where the temperature dependence (both of diameter D and frequency $f(D)$) of asphaltene colloidal aggregates dissolved in resins was studied. As shown below, diameter frequency (relative concentration of particles with diameter D), changed with temperature according to particle size. For the biggest (D_B), a continuous decrease in $f(D_B)$ was observed whereas for the smallest (D_S) a continuous increase in $f(D_S)$was observed. However, for intermediate sized particles, $f(D_I)$ went through a maximum suggesting that conversion to small particles meets a energy barrier high enough to produce accumulation of medium sized particles or aggregates. As discussed below, these results strongly suggest that small particles are actually A1 molecules which because of their low solubility are difficult to be released from the medium-sized aggregates.

Experimental Details

Asphaltenes were isolated from furrial and DM-153 crude oils by addition of 40 volumes of *n*-heptane using the IP-130 standard as described earlier.[8] The precipitated solid, containing asphaltene and resins, was transferred to a paper thimble, placed in a Soxhlet liquid−solid extractor, and resins were removed with boiling *n*-heptane during a period of three days. After this period, resins were recovered after n-heptane distillation under vacuum and used for preparation of the resins−asphaltene mixtures.

Asphaltene−resins homogeneous mixtures, 3% asphaltene in resins, were prepared by dissolving both components in chloroform. The resulting solution was sonicated for 0.5 h, and the chloroform was evaporated under vacuum.

Preparation of samples at different temperatures was achieved by transferring the asphaltene−resins mixture (0.5 g) to a glass vial and placing the vial within a Parr reactor of 100 mL capacity (series 4590). A sample holder was also placed within the reactor. The sample was contacted with a thermocouple type *J*, the reactor was closed, and the contents were heated during a period of 6 h under nitrogen atmosphere (at initial pressure). Temperatures in the 25−250 °C range were used. After this time, the reactor was opened and a small amount of sample was placed in sample holder, and the sample holder was quickly frozen in undercooled nitrogen (a slurry of liquid and solid nitrogen) and kept in this conditions until needed for the freeze fracture experiment.

Freeze fracture experiments were carried out in a JEOL apparatus model 9010C. Samples were fractured at −150 °C under high vacuum (10^{-6} Torr), as described earlier.[39] Briefly, the frozen sample is fracture after being hit by a sharp bladed cooled at the same temperature (−150). In this way, the solid sample is broken in two halves one of which remaining at the sample holder and the other is blown away. The surface produced after the fracture, is then shadowed with platinum atoms sprayed on the surface at 45° with respect to the sample holder normal to produce contrast and after that sprayed at 90° with carbon powder to increase mechanical resistance. The combined spraying produces a layer that replicates the topography of the surface. After these procedures, the apparatus is brought to atmospheric pressure, the frozen sample is withdrawn, and placed in a flask containing toluene, where all the organic

(34) Pereira, J. C.; López, I.; Salas, R.; Silva, F.; Fernández, C.; Urbina, C.; López, J. C. Resins: The molecules responsible for the stability/instability phenomena of asphaltenes. *Energy Fuels* **2007**, *21* (3), 1317–1321.

(35) Leon, O.; Contreras, E.; Rogel, E.; Dambakli, G.; Espidel, J.; Acevedo, S. The Influence of the Adsorption of Amphiphiles and Resins in Controlling Asphaltene Flocculation. *Energy Fuels* **2001**, *15* (5), 1028–1032.

(36) Douda, J.; Llanos Ma, E.; Alvarez, R.; Navarrete Bolanos, J. Structure of Maya Asphaltene-Resin Complexes through the Analysis of Soxhlet Extracted Fractions. *Energy Fuels* **2004**, *18* (3), 736.

(37) Carnahan, N. F.; Salager, J.-L.; Anton, R.; Davila, A. Properties of Resins Extracted from Boscan Crude Oil and Their Effect on the Stability of Asphaltenes in Boscan and Hamaca Crude Oils. *Energy Fuels* **1999**, *13* (2), 309–314.

(38) Gonzalez, G.; Neves, G. B. M.; Saraiva, S. M.; Lucas, E. F.; dos Anjos de Sousa, M. Electrokinetic Characterization of Asphaltenes and the Asphaltenes-Resins Interaction. *Energy Fuels* **2003**, *17* (4), 879–886.

(39) Acevedo, S.; Rodriguez, P.; Labrador, H. An electron microscopy study of crude oils and maltenes. *Energy Fuels* **2004**, *18*, 1757–1763.

(40) Acevedo, S.; Escobar, O.; Echevarría, L.; Gutierrez, L. B.; Mendez, B. Structural Analysis of Soluble and Insoluble Fractions of Asphaltenes Isolated Using the PNP Method. Relation Between Asphaltene Structure and Solubility. *Energy Fuels* **2004**, *18*, 305–311.

material is dissolved leaving the C−Pt replica. This replica is then placed in the grid sample holder and analyzed by TEM.

TEM measurements of replicas were performed using a JEM 1220 equipment with an accelerator voltage of 110 kV. Microphotographs were taking with 50000X augment. This was increased 2-fold after photo development.

Diameter and particle density were determined using the Scion Image Windows program (SIWP; see below).

The number of particles in 100 nm^2 was determined by counting the number of particles present in a 10 × 10 square of 100 nm sides.

The volume of a particle was calculated using the ellipsoidal equation

$$V = \frac{4}{3}\pi abh \quad (1)$$

In this equation, a is the length of the semiaxis measured perpendicular to the particle shadow; b is the length of the semiaxis measured parallel to the particle shadow; and h is the length of the semiaxis corresponding to the particle height. A simple trigonometric relation (tan(45) = h/s) was used to obtain h, where s is the length of the shadow measured from the center of the particle; since, tan(45) = 1, $h = s$, accordingly.

Results

Figure 1 is an example of the procedure employed to measure the diameters and diameter densities. The scale mark in the photograph, equal to 500 nm, is clearly shown. The inset corresponds to the visualization of the SIWP with a scale in nanometers (horizontal) and a vertical scale measuring contrast. The strong band on the left of the inset corresponds to the measurement of particle and neighborhood indicated by the inclined line to the right of the inset. Unless stated otherwise, diameters measured perpendicular to the shadow are the ones referred to in this work. By virtue of the developing process, photograph "shadows" appear bright in the positive of the photos being measured. In this way, particles were measured one by one to obtain the results described below.

Errors in measurements were estimated at ±0.4 nm by evaluating differences between samples of 60 or more particles of different diameters.

For convenience, diameters in Table 1 are plotted as a function of temperature in Figure 2.

Inspection of Tables 1 and 2 shows that no significant change in D_M was observed above 200 °C. This, together with the constant value observed for D_m suggests that the system is approaching boundaries regarding diameter range. The constant value observed for D_m above 100 °C could be due in part to limitation of the method to detect particles below this size. However, according to data by Tanaka described above,[33] mean diameters of this size were reported at 300 °C.

Particle density, defined here as the number of particles in 10^4 nm^2, were 20 ± 1 for furrial and 19 ± 1 for DM-153 samples. These values were the average of ten different measurements in ten different sections of the image. No significant dependence of this density values with temperature was observed.

A sample of diameters measured at 100 °C for the DM-153 is shown in Table 3 where 61 particles were measured. Due to limitations in image processing, differences in consecutive diameters can not be measured with a precision smaller than 0.8 nm. Very similar results were obtained for other temperatures and for the other sample (furrial).

In Figures 3 and 4, frequency of diameter values $f(D)$ were plotted against temperature. For convenience, $100f(D)$ was plotted in these figures. These values were obtained at each temperature and each diameter as shown in Table 4.

The number of particles with diameter D, N_D (second column in Table 4), were counted, and this was divided by the total number of particles (61 in this example) to obtain $f(D)$. Multiplication by 100 afforded the values in the last column of

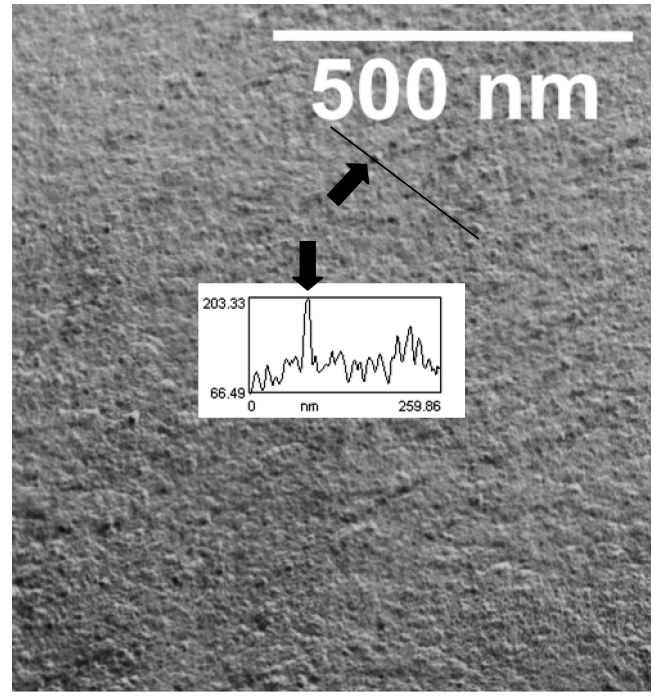

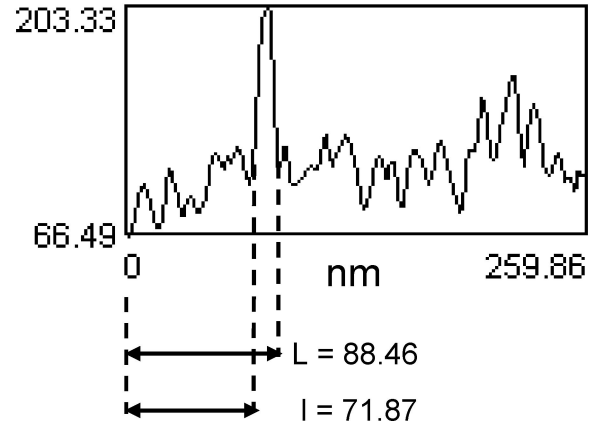

Figure 1. Electron photomicrograph showing the way that a particle size is measured over a freeze fracture replica. On the image, arrows are pointing both to the particle and contrast profile.

Table 1. Mean Diameter D_p and Other Parameters Measured for the Resins−Asphaltene Mixtures at Several Temperatures with a Sample of Furrial[a]

temp (°C)	D_p	σ^b	$D_M{}^c$	$D_m{}^d$
25	5.2	1.03	8	3
75	4.7	0.9	7.6	3.4
100	4.7	0.77	7.6	3.4
125	4.5	0.76	6.7	3.4
150	4.2	0.73	5.9	2.5
175	4.0	0.65	5.9	2.5
200	3.8	0.61	5.0	2.5
225	3.7	0.6	5.0	2.5
250	3.5	0.58	5.0	2.5

[a] All diameters and standard deviations are in nanometers; error is better than ±0.5 nm. [b] Standard deviation of size distribution. [c] Maximum diameter observed. [d] Minimum diameter.

ohio2/yef-yef/yef-yef/yef99907/yef2932d07z | xppws | 23:ver.3 | 6/7/08 | 22:03 | Msc: ef-2008-00108p | TEID: kkt00 | BATID: ef5a04

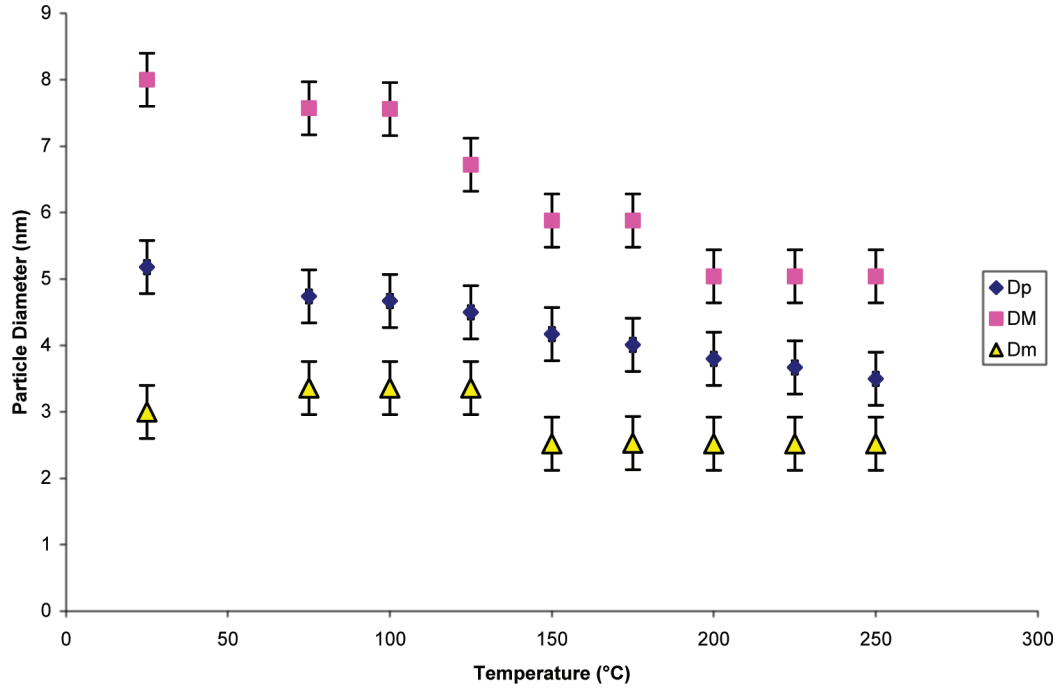

Figure 2. Change of particle diameters with temperature, for average (D_P), maximum (D_M), and minimum (D_m) diameters. Diameter errors are estimated at ±0.4 nm. Sample: Furrial.

Table 2. Mean Diameter D_p and Other Parameters Measured for the Resins−Asphaltene Mixtures at Several Temperatures with a Sample of DM-153[a]

temp (°C)	D_p	σ^b	$D_M{}^c$	$D_m{}^d$
25	5.1	1.27	10.00	3.00
75	4.8	0.9	7.6	2.8
100	4.6	0.84	6.8	2.5
125	4.3	0.8	5.9	2.5
150	4.1	0.77	5.9	2.5
175	3.9	0.73	5.9	2.5
200	3.7	0.7	5.0	2.5
225	3.5	0.66	5.0	2.5
250	3.3	0.64	5.0	2.5

[a] All diameters and standard deviations are in nanometers; error is better than ±0.5 nm. [b] Standard deviation of size distribution. [c] Maximum diameter observed. [d] Minimum diameter.

Table 3. Sample of Particles Observed for DM-153 at 100 °C

particle diameter (nm)	absolute frequency	difference (nm)
2.5	1	
3.4	7	0.9
4.2	27	0.8
5.1	18	0.9
5.9	6	0.8

Table 4. This procedure was repeated for each temperature considered to obtain Figures 3 and 4.

As written in the discussion below, the $f(D)$ curves in Figures 3 and 4 could be described in terms of a consecutive process where big aggregates are converted to medium ones which in turn are converted to smaller aggregates and molecules. The maximum obtained (as the case for 4.2 nm particles in Figure 3 and the 3.5 particle in Figure 4) implies that the consecutive process have not reached equilibrium. As described in the Experimental Details section, each sample analyzed was kept at the selected temperature for a period of 6 h.

Due to limitations of the FF technique, accurate calculations of molar volumes cannot be determined. However, an estimation of molar volume could be done for the case where the 2.5 nm particle is a solvated molecule with a disk or oblate ellipsoidal shape. The thickness of this disk could be estimated from Bardon et al. data where thickness in the 0.8−1 nm range were reported.[31] According to Tanaka et al.[33] (see above) and to molecular mechanics calculations,[40] van der Waal distances between asphaltenes[33] or asphaltenes models[40] is not less than 0.35 nm. Accordingly, a solvation shell thickness close to 0.35 could be assumed. With these data and results, a volume could be calculated from equation ellipsoidal 1:

$$V_a = \frac{4}{3} N_A 10^{-21} \pi r^2 t \qquad (2)$$

Here V_a is the molar volume of the asphaltene molecule, N_A is Avogadro's number, 10^{-21} is the factor to convert cubic meters to cubic centimeters, r is the ellipsoidal radius, and t is the thickness. Substitution of $t = 0.8$ nm leads to eq 3

$$V_a = \frac{4}{3} \pi N_A 10^{-21} \left(\frac{2.5 - 0.7}{2}\right)^2 0.8 \qquad (3)$$

As described in the paragraph above, the constant 0.7 (equal to 0.35 × 2) is included to subtract the solvation shell provided by resins molecules. One solvation layer is assumed as well as a van der Waals distance of 0.35 nm between asphaltene and resins (see ref 12). After substitution a $V_a \approx 1600$ cm^3 is obtained which is equal to the molecular mass for a sample with a density equal to 1. Using laser desorption mass spectrometry methods (LDI MSM) and FD MS, molecular mass (MM) in this range has been reported recently in the literature both for asphaltenes[41,42] and heavy petroleum molecules.[43] However, according to similar LDI MS studies performed by several research groups,[45–47] asphaltenes and other petroleum products react under the effect of the laser affording too high MM. This interesting debate is somewhat outside the scope of this work.

In any case, we should keep in mind that small changes within the experimental error of the present FF-TEM technique could

ohio2/yef-yef/yef-yef/yef99907/yef2932d07z | xppws | 23:ver.3 | 6/7/08 | 22:03 | Msc: ef-2008-00108p | TEID: kkt00 | BATID: ef5a04

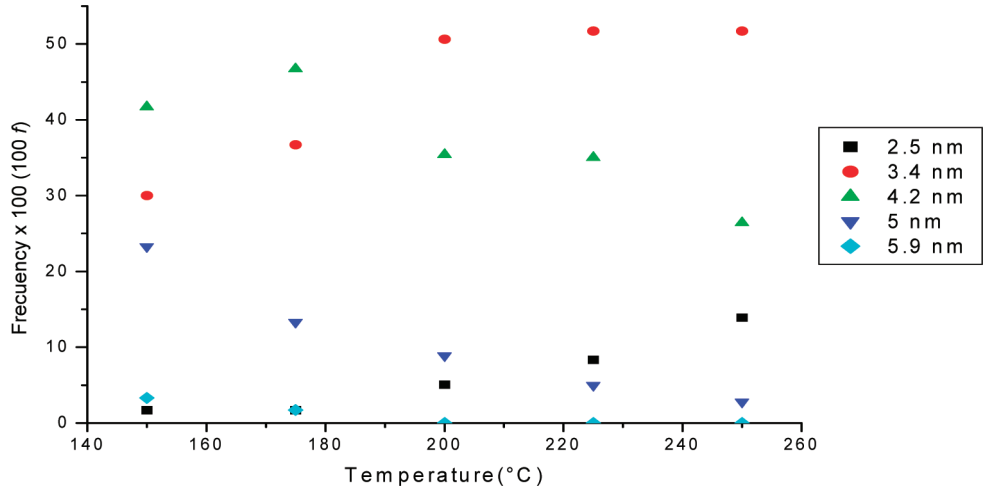

Figure 3. Plot of frequency against temperature for DM-153 system. Frequency values *f*(*D*) were calculated as described in Table 4.

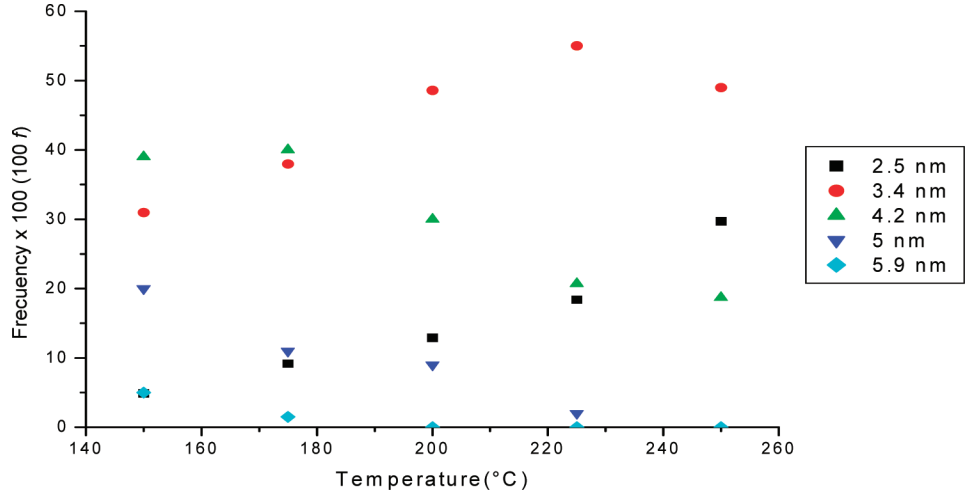

Figure 4. Plot of frequency against temperature for furrial system. Frequency *f*(*D*) were calculated as described in Table 4.

Table 4. Calculation of 100*f*(*D*) Values at 150 °C with a Sample of DM-153

D	N_D[a]	100*f*
2.6	3	4.9
3.4	19	31
4.2	24	39
5	12	20
5.9	3	5

[a] Number of particles with diameter *D*.

lead to large changes in V_a values calculated from eq 2 above, and hence, we will not pursue this matter any further.

Discussion

The resins−asphaltene mixtures studied here are very convenient both from practical and theoretical points of view. Being a very low volatile sample, it can be studied at the high temperatures used here without any major concern for evaporation during handling. The mixtures were highly homogeneous leading to solutions without any evidence of phase separation as can be tell by looking at the TEM photos (see Figure 1). At all temperatures tried, the mixtures could be properly handled for their transference to the sample holder and were conveniently frozen to afford very good fractures. From a theoretical point of view, dispersion of asphaltenes by resins is a very well-known fact[34–38] and stable solution could be expected at high temperatures. As described in the review above stable particles, probably stabilized by resins, have been observed at high and low temperatures[17,32] and particle diameters were found to decrease with resin content.[31]

In particular, under the high temperature conditions and low asphaltene concentration employed here, any asphaltene aggregate is expected to be dissociated by resins and this is strongly suggested by the results shown in Figures 3 and 4.

(41) Acevedo, S.; Gutierrez, L. B.; Negrín, J. G.; Pereira, J. C.; Mendez, B.; Delolme, F.; Dessalces, G.; Broseta, D. Molecular weight of petroleum asphaltenes: A comparison between mass spectrometry and vapor pressure osmometry. *Energy Fuels* **2005**, *19*, 1548–1560.

(42) Tanaka, R.; Sato, S.; Takanohashi, T.; Hunt, J. E.; Winans, R. E. Analysis of Molecular Weight Distribution of Petroleum Asphaltenes Using Laser Desorption-Mass Spectrometry. *Energy Fuels* **2004**, *18*, 1405–1413.

(43) Quian, K.; Edwards, K. E.; Siskin, M.,; Olmstead, W. N.; Mennito, A. S.; Dechert, G. J.; Hoosain, N. Desorption and Ionization of Heavy Petroleum Molecules and Measurements of Molecular Weight Distribution. *Energy Fuels* **2007**, *21*, 1042–1047.

(44) Sheu, E. Y. Small angle scattering and asphaltenes. *J. Phys.: Condens. Matter* **2006**, *18* (36), S2485–S2498.

(45) Smith, D. F.; Schaub, T. M.; Rahimi, P.; Teclemariam, A.; Rodgers, R. P.; Marshall, A. G. Self-Association of organic acids in petroleum and Canadian bitumen characterized by Low- and High-Resolution Mass Spectrometry. *Energy Fuels* **2007**, 1309–1316.

(46) Hortal, A. R.; Martínez-Haya, B.; Lobato, M. D.; Pedrosa, J. M.; Lago, S. On the determination of molecular weight distributions of asphaltenes and their aggregates in laser desorption ionization experiments. *J. Mass Spectrom.* **2006**, *41*, 960–968.

(47) Hortal, A. R.; Hurtado, P.; Martinez-Haya, B.; Mullins, O. C. Molecular-Weight Distributions of Coal and Petroleum Asphaltenes from Laser Desorption/Ionization Experiments. *Energy Fuels* **2007**, *21* (5), 2863–2868.

These results could be conveniently discussed in terms of the following consecutive scheme:

$$\mathrm{Ag(B)} \xrightarrow[T]{k_1} \mathrm{Ag(M)} \xrightarrow[T]{k_2} \mathrm{(S)}$$

In this scheme, Ag stands for asphaltene aggregate and the letters B, M, and S stand for big, medium, and small, respectively. The letter *S* stands for a small entity which will be defined below. The scheme implies that at any temperature considered Ag(B), Ag(I), and S are present and that *f*(*D*)is displaced toward lower diameters as the temperature is increased (see the Experimental Details). Thus, as the temperature is increased, the frequency of Ag(B) is depleted and at the same time frequency as S increases (see Figures 3 and 4). Maxima in $f(D)-T$ curves could be expected for intermediates Ag(M) because they appear from larger species and disappear to afford smaller ones, *and when doing so, they do it at different rates*. In other words, at each temperature examined, conversion to small entities

$$\mathrm{Ag(M)} \xrightarrow[T]{k_2} \mathrm{(S)}$$

appear to have a conversion rate k_2 lower than k_1 corresponding to conversion

$$\mathrm{Ag(B)} \xrightarrow[T]{k_2} \mathrm{Ag(M)}$$

This would lead to the observed accumulation of Ag(M) (see the *f*(3.4) and the *f*(4.2) frequency curves in Figures 3 and 4). On the other hand, no diameter less than 2.5 nm could be measured and these two results strongly suggest that the small entities observed are asphaltene molecules. Moreover, they suggest that these molecules belong to the low soluble fraction A1, simple because those in A2 are soluble in resins. Thus, the second step above could be written as

$$\mathrm{Ag(M)} \xrightarrow[T]{k_1} \mathrm{A1M}$$

In view of the low solubility of A1, this step is expected to meet a energy barrier higher that the first, leading to accumulation of the intermediary aggregates Ag(M) and $k_1 > k_2$.

These argument are coherent with the fact that extreme dilution is needed to avoid asphaltene aggregation.[1–3]

Of course, all aggregates in the above colloidal solutions are expected to be promoted by molecules in fraction A1. In other words, aggregates or colloidal particles would have the A1A structure described above and previously.[8,9] In the present case, resins play the role of solvent.

Also within the present experimental error (±0.4 nm) molecules of 2.5 nm would span a wide range of MM values (see the volume estimation above).

It is interesting to mention that the asphaltene stacking referred to above,[18] and reported long ago by Yen,[48] should be mainly constituted by A1M or CTM simply because they would be expected to pack efficiently and to afford crystalline-like or solid (colloidal) phases detectable by XRD, SANS, SAXS, and the present FF-TEM methods. We believe that matter related to these techniques and to the size and shape of colloids, such as these reviewed above,[10–12,17–20,24–26,28,29,31–33,39] are related to the presence of A1-type molecules. These are responsible by the colloidal phase or for aggregates whereas the A2-type or ATM would be in solution and acting as a dispersant for the A1 colloids or aggregates. A similar conclusion was reported by Evdokimov[3] (see comments in the Introduction section).

A final comment regarding the smallest size we measured in this work; as described above, we believe that particles in this size range are molecules. This size (2.5 nm) is larger than the one reported by Mullins et al.[4a] As described above, these authors reported a hydrodynamic radius of 1 or a 2 nm in diameter. The somewhat small difference (0.5 nm; ±0.4 nm our experimental error) could be accounted for in terms of the following arguments: Under the high dilution used by these authors (0.03−3.0 mg/L), no aggregates are expected. Hence, both A1M and A2M would be in solution. As reported earlier, no significant MM differences were found between A1 and A2 when examined by LDI MS methods.[41] However, A2M, being flexible, would produce folded conformers with a smaller hydronamic radius than A1M.[8,9,40] Hence, the hydronamic radius of the A1 + A2 mixture (asphaltenes, such as the one reported in ref 4a) would be smaller than the one corresponding to rigid A1M.

Conclusions

The results presented suggest very strongly that, in the asphaltene−resin solutions studied here, asphaltenes aggregates of different size are present in solutions along with A1M at temperatures above 100 °C. The results are consistent with the hypothesis above where A1M forms the medullar part of the aggregate or colloid dispersed by A2M and resins. Due to low solubility of A1M, dissociation of small aggregates to afford A1M is a difficult step which leads to accumulation of intermediate sizes in a process that could be represented by the following consecutive process

$$\mathrm{Ag(B)} \xrightarrow[T]{k_1} \mathrm{Ag(M)} \xrightarrow[T]{k_2} \mathrm{A1M} \quad \text{where } k_1 > k_2$$

The suggested molecular diameter of A1M was found to be comparable to other reported, and the proposed A1A colloidal model was found to be consistent with present results and with data reported in the literature.

Acknowledgment. The financial support provided by projects FONACIT (G2005000430) and CDCH (AI-03-12-5509-2004, PG-03-00-5732-2004, PI-03-00-5648-2004) is gratefully acknowledged. We also thank Lic. Betilde Segovia for typing the manuscript and the Laboratorio de Polímeros, Universidad Simón Bolívar, for kindly providing TEM facilities.

Nomenclature

A1 = asphaltene fraction of very low solubility in toluene at room temperature (close to 0.09 g/L)
A2 = asphaltene fraction soluble in toluene at room temperature; solubility in the 57−100 g/L range depending on sample
A1A = aggregates or colloids formed by A1M where the medullar part or core is occupied by A1M and the periphery is occupied by A2M and solvent
A1M = molecules in the A1 fraction, represented by rigid condensed polynuclear systems models with alkyl substituents on the molecule periphery[9,40]
A2M = molecules in A2 fraction represented by flexible structure where polycyclic units are connected between them by alkyl chains[9,40]
Ag(B), Ag(I) = big and intermediate aggregates
ATM = archipelago-type molecules similar to A2M
B = big particle (D > 4 nm)

(48) Yen, T. F. Structural Differences Between Asphaltenes Isolated from Petroleum and Coal Liquid. In *Chemistry of Asphaltenes*; Bunger, J. W., Li, C. N., Eds.; Advances in Chemistry Series; American Chemical Society: Washington, DC, 1981; Chapter 2, p 29.

CTM = continental-type molecules similar to A1M
D = diameter of particle
$f(D)$ = frequency of particles of diameter D
FD MS = field desorption mass spectrometry
FF-TEM = freeze fracture transmission electron microscopy method
I = particle of intermediate size; between big (5 nm or higher) and small (2.5 nm)
k_1 = rate constant of the step corresponding to conversion of big particles to intermediate particles
k_2 = rate constant of the step corresponding to conversion of intermediate particles to A1 molecules
LDI MS = laser desorption mass spectroscopy
MM = molecular mass
S = small particle (2.5 nm); here considered as molecules
SANS = small angle neutron scattering
SAXS = small angle X-ray scattering
SIWP = Scion Image Windows program; used for image digitalization and measurement of particle diameters
T = temperature
V_a = molecular volume of asphaltene
XRD = X-ray diffraction

EF800108P